Long-Lived Foams Stabilized by a Hydrophobic Dipeptide Hydrogel

DOI: 10.1002/ ((please add manuscript number))
Article type: Full Paper

Long-Lived Foams Stabilized by a Hydrophobic Dipeptide Hydrogel

Tao Li, Fabio Nudelman, Joe W. Tavacoli, Hugh Vass, Dave J. Adams, Alex Lips and Paul S. Clegg*

T. Li, Dr. J.W. Tavacoli, H. Vass, Prof. A. Lips, Dr. P.S. Clegg
School of Physics and Astronomy, University of Edinburgh, Peter Guthrie Tait Road, Edinburgh EH9 3FD, UK
E-mail: paul.clegg@ed.ac.uk
Dr. F. Nudelman,
School of Chemistry, University of Edinburgh, Joseph Black Building, David Brewster Road, Edinburgh EH9 3FJ, UK.
Prof. D. J. Adams,
Department of Chemistry, University of Liverpool, Crown Street, Liverpool, L69 7ZD, UK

Keywords: supramolecular materials, dipeptide fibers, hydrogel, self-assembly

A hydrogel of hydrophobic dipeptides can be used to create a wet foam with long-term stability. The dipeptide molecules self-assemble into fiber-like networks (due to the presence of metal ions) both at air-water interfaces and in the continuous phase. The former creates an interfacial film stabilizing the air bubbles while the latter forms a bulk gel, which prevents bubble movement and retards growth. If the storage modulus (G') of the bulk hydrogel is sufficiently high it can stop the coarsening of the air bubbles and thus dramatically improve the stability of the foam. Cryogenic scanning electron microscopy (cryo-SEM) and Raman spectra reveals the width of the fibers (200 nm) and that they are held together by hydrogen bonds. In the absence of bubbles, phase separation is observed between a hydrogel and a water-rich phase; in the foam this can be suppressed provided that the concentration of dipeptides and metal ions are sufficiently high. We speculate that the resistance of the bubble arrangement to compaction and hence further drainage arrests the process of phase separation. This foam system has the advantages of long stability, low cost, as well as easy preparation; therefore, it has potential applications in food manufacturing, drug delivery and personal care industries.

1. Introduction

Wet foams have attracted broad interest in part because of their numerous different applications, including some food products, use in mineral extraction, and the development of new porous materials.[1–3] For many of these applications, the foam stability is an important characteristic.[4, 5] However, foams are thermodynamically unstable, and can be easily destroyed by coarsening and coalescence. As a result, long-term stabilization of wet foams is a critical problem. Some progress has been made over the last twenty years: earlier reports investigated the role of surfactants in improving the foam stability;[6, 7] more recently, colloidal particles have been used to increase the lifetime of wet foam.[2, 8, 9] Some related investigations show that rod-like (or fiber-shape) particles exhibit outstanding stabilizing properties because of the formation of a thick protective shell around the air bubbles by entanglement and overlapping of the rods (or fibers).[8]

Besides surfactants and colloidal particles, polymers, proteins and peptides are also considered to be attractive stabilizers for wet foams.[10] For example, both egg white proteins and milk proteins are well known for their efficient foam production.[11, 12] Compared with the unhydrolyzed proteins, peptides can markedly improve foam-ability and foam stability, due, in part, to the reduced size of peptides promoting a more rapid adsorption at the interface.[13, 14] In previous studies, some functional peptides have been designed to form interfacial ensembles that can act as environmentally friendly foaming agents.[10, 15] Their foaming properties were shown to be influenced by ionic strength, pH and temperature of the foaming solution,[16] as well as the relative hydrophobicity of the peptides.[17] Because of the low-cost production and inherent biodegradability, peptides open up the possibility of functional biosurfactant-stabilized foams.[18, 19]

To stabilize a wet foam, peptides either need to be gelled in the continuous phase between the air bubbles or they need to form a rigid layer on the bubble surfaces or both. Furthermore, it is required that an, initially gelled, continuous phase can be melted to allow foaming and re-gelation to suppress drainage or coalescence.[5]

Very recently, we have shown that hydrophobic dipeptide molecules (NapFF and BrNapFF) can self-assemble into an elastic gel film at the air-water interface. By drop-casting a dipeptide in a high pH solvent onto a liquid subphase at low pH, the carboxylic acid becomes protonated which induces gelation at the interface.[20] We have also demonstrated that the interfacial layer can be used to stabilize large air bubbles (millimeter-size) for days at least.[20] These features strongly suggest that the dipeptide hydrogel would be an excellent candidate for foam and emulsion stabilization. Ulijn and coworkers have stabilized oil-in-water and water-in-oil emulsions by self-assembling dipeptides at the organic/aqueous interface. Superior long-term stability of the emulsions has been observed.[21] However, no studies have been carried out on foams stabilized by dipeptide hydrogels so far.

Besides a pH change, temperature and metal ions can also lead to the formation of a hydrogel. For foam studies, metal ions are preferable. First of all, doubly charged metal ions efficiently promote the gelation of dipeptide fibers giving the high storage moduli (G') of the gels which have been observed using rheological measurements.[22] Secondly, using metal ions avoids the addition of other liquid (*e.g.* aqueous HCl) and increases the normalized foam volume. (This is also true for gelation using a change in temperature.[23]) Moreover, a hydrogel induced by metal ions can be prepared at a broad range of pHs; in particular, this expands the range of dipeptide-based gelators that can be used at physiological pH.[24] In this article, we report that a hydrogel of self-assembled NapFF dipeptides (similar to that used in ref. [25]) can stabilize a wet foam for weeks. Here, metal ions are used to induce the gelation; we demonstrate that the foam

stability is related to the concentration of dipeptide molecules. Curiously, not only does the dipeptide gel stabilize the foam, the air bubbles also suppress the phase separation of a hydrogel phase and a water-rich phase. Raman spectra are used to study the secondary structure of these self-assembled molecules while cryo-SEM reveals the fiber-like networks which stabilize the foam. Finally, we demonstrate the dramatic effect of different metal ions on gelation and the resulting foam properties.

2. Results and discussion

Figure 1 illustrates the foam prepared by adding $CaCl_2 \cdot 2H_2O$ (35 mg/mL) into a NapFF (8 mg/mL) foaming solution and then aerating with a homogenizer. The foam can be stabilized for more than two weeks with only very modest drainage (Figure 1b-f). A small amount of liquid phase can be seen at the bottom of the vial. A photograph of the appearance of the wet foam is given in Figure 1g: it can be extruded and shaped with a pipette demonstrating that it exhibits a yield stress. The mechanical properties are further demonstrated in Figure 1h. Here the storage and loss moduli are presented as the frequency of the oscillating shear is varied. The storage modulus, G', is always significantly larger that the loss modulus, indicating that the foam has gel-like properties.

One potential stabilization mechanism provided by the dipeptide hydrogel is the formation of a viscoelastic physical network in the continuous phase, *i.e.*, the hydrogel delays drainage and protects the air bubbles against coalescence or coarsening.[26] An additional mechanism stems from the presence of a viscoelastic network of self-assembled dipeptides on the surface of the bubbles. Cryo-SEM was used to visualize the viscoelastic network without disrupting the structures (**Figure 2a**). Figure 2b shows the spectacular fibrous networks at the interface. Averaged over more than 50 fibers, we find that the width of a single fiber is approximately

190±50 nm. This is markedly thicker than the strands in the interfacial films we created at the air-water interface[20] and is also thicker than strands in bulk hydrogels.[22] In the continuous phase, excess dipeptides can be flocculated and form a three-dimensional network, which keeps the bubbles well separated. These fibrous aggregates can also be observed with cryo-SEM (Figure 2c, d) and confocal microscopy (Figure 2g). For the confocal image of the air bubbles inside a freshly prepared foam, Figure 2g, the dipeptide dispersions were labeled with Thioflavin T (ThT). The observed ThT fluorescence enhancement demonstrates the presence of the self-assembled dipeptides with possible β-sheet order at the surface of the bubbles. Most of the bubbles are spherical (average diameter of ~100 μm). By contrast, the foamability of ungelled NapFF solution is very low: the resulting foam is stable for less than 2 hours (Figure S1).

The secondary structure of the fibrous networks has been characterized by Raman spectroscopy following a drying step (Figure 2h). The weak peak at 1675 cm^{-1} could be indicative of β–sheet formation; a related peak has been observed in FTIR spectra of the interfacial films at the air-water interface.[20] The bands at 1003 cm^{-1}, 1030 cm^{-1}, 1205 cm^{-1}, 1583 cm^{-1} and 1602 cm^{-1} are all associated with the phenylalanine groups.[27] The bands at 772 cm^{-1}, 1390 cm^{-1}, 1446 cm^{-1}, 1468 cm^{-1} and 1632 cm^{-1} are close to those of molecular naphthalene.[28] These strong sets of peaks from the aromatic groups might suggest that they are relatively free to vibrate within the hydrogel. Indeed the 1003 cm^{-1} phenylalanine peak has been used extensively as a signature that phenyl groups are exposed and free to vibrate.[29] We tentatively infer that the self-assembly might be driven primarily by hydrogen bonding between the dipeptide molecules with little role for π-π stacking in these interfacial systems. Besides the dipeptides self-assembled at the interface and in the continuous phase, excess molecules are found in the water-rich phase at the bottom of the vial, where the fluorescence signal from naphthalene can be measured (Figure S2).

In our foam system, it appears likely that both the interfacial films and the bulk hydrogel are involved in conveying stability to the system. We have previously demonstrated that interfacial films prepared from hydrophobic dipeptides can give long term stability to bubbles.[20] In the foam system, the interfacial film crucially prevents coalescence when two bubbles are pushed into one another. Next we consider in more detail the role of the continuous phase: here the bulk gel with a high storage modulus (*G'*) influences whether the bubbles can change size. In Figure S3a we show the storage, G', and loss, G", moduli for the original hydrogels (no bubbles). We assume that the gel retains its native characteristics between the bubbles. If *G'* is smaller than the Laplace pressure (P_L), gas from the smaller bubbles (with a larger P_L) can escape and diffuse through the continuous phase to the lower pressure, larger bubbles. When *G'* is greater than P_L, bubbles cannot change size and hence, the gas transfer can be slowed down and eventually stopped. For a bubble of 120 μm diameter, P_L is about 10^3 Pa, while *G'* of a NapFF gel induced by Ca^{2+} is about 10^5 Pa.[30] As a result, the foam can be stabilized for weeks without obvious coarsening and coalescence.

To stabilize the foam system, a high concentration of dipeptide is required, although ultimately some of the molecules can be found with the drained solvent. **Figure 3**a and 3b are foams with lower NapFF concentration (but the same concentration of $CaCl_2 \cdot 2H_2O$, see experimental section). For 5 mg/mL NapFF system, drainage occurs by the second day after preparation. Water-rich phase leaks out of the foam macroscopically, causing the appearance of some large, irregularly shaped air pockets (Figure 3a). As a result, the volume of foam decreases whereas the volume of liquid phase increases. After two weeks, the foam separates from the vial wall and floats on the surface of the drained liquid. In 2 mg/mL NapFF system, the fibers are much thinner (~40 nm in diameter, Figure 2e) and the foam collapses in only one week (Figure 3b). Figure 3c shows confocal images of the air bubbles from the aging 5 mg/mL system. During

the separation / drainage process, most bubbles are no longer spheres and tend to be pushed into one another and hence distorted. Additionally, the hydrogel between the bubbles begins to become visible via the ThT fluorescence. This phenomenon becomes more obvious 50 days after the foam formation, with more aggregates of dipeptides appearing between the bubbles (see below). We note that although there is a wide bubble size-distribution, the average diameter of the air bubbles remains unchanged during the drainage process, which means very little coalescence or coarsening takes place.

Reducing the concentration of metal cations can also affect the foam stability. The foam height recorded as a function of time with different amounts of $CaCl_2 \cdot 2H_2O$ is given in **Figure 4a**. The height decreases noticeably within the first few hours and then remains approximately the same for more than two weeks. Evidently, the final height of the foam depends on the concentration of metal ions. Drainage / phase separation has been observed in samples with lower metal ion concentration (Figure 4b and c). Again, no obvious coalescence and coarsening occur during the drainage process.

In order to establish the origin of the decrease in foam volume (Figure 4), the bulk phase behavior of the hydrogel (no bubbles) with different amounts of NapFF and $CaCl_2 \cdot 2H_2O$ was investigated. As shown in **Figure 5**, phase separation of the hydrogel and the surplus aqueous phase occurred within 10 minutes for all compositions. (In the case of Figure 5a this initial change in volume is of the same order as the initial loss of foam height, Figure 4). When the concentration of NapFF or Ca^{2+} was reduced, the volume of the hydrogel phase decreased. However, during the following two weeks of observation, any further shrinkage in any of these gel samples was insignificant. After six months each of the hydrogels had noticeably decreased in volume: those in Figure 5a and 5c by about 10%; the hydrogel in Figure 5b had undergone a more pronounced loss of volume (about 40%) and had begun to pull away from the sides of the

vial. Figure 5d and 5e show that a hydrogel induced using $MgSO_4$ also undergoes significant shrinkage over a six month period.

The bulk phase separation behavior presented in Figure 5 can now be compared to the aging of the foam. The hydrogel in Figure 5a has the same composition (8 mg/mL NapFF; 35 mg/mL $CaCl_2 \cdot 2H_2O$) as the foam in Figure 1b and the foam height data in Figure 4a (black squares). Evidently, the initial loss of height of the foam could be an attenuated version of the phase separation of the bulk hydrogel. However, the steady but unspectacular loss in height of the foam over subsequent days has no counterpart in the bulk hydrogel behavior. Instead this is presumably due to slow rearrangements of bubbles leading to compaction as frequently occurs during foam aging.[31] The hydrogel in Figure 5b has the same composition (8 mg/mL NapFF; 4.4 mg/mL $CaCl_2 \cdot 2H_2O$) as the foam in Figure 4b and the height data in Figure 4a (red circles). For this composition there is no equivalent in the foam of the immediate loss of ~30% of the hydrogel volume. Instead there is a steady loss of foam volume over many days. What slows the phase separation in this case (Figure 5b) and attenuates the volume change for Figure 5a? Adsorption of the dipeptide strands onto the bubble surfaces will reduce the effective concentration of dipeptide in the spaces between the bubbles. By comparing Figure 5a and Figure 5c, we suggest this would only serve to make phase separation more pronounced. By contrast, the fixed volume of the hydrogel-rich phase, enforced by the arrangement of bubbles, may prevent (arrest) complete phase separation. The consequence is a foam sample with a composition which would be unstable for a bulk hydrogel. Some phase separation may occur over time associated with the compaction of the bubbles, with hydrogel forming between the bubbles. This compaction picture is backed up by the imaging data in Figure 3c which shows additional structure appearing in the continuous phase as the foam ages. Under the same conditions, BrNapAV (a relatively hydrophilic dipeptide that forms spherical structures at high

pH rather than worm-like micelles)[24] cannot form any network to stabilize the foam (Figure S4); neither at the interfaces nor in the continuous phase.

Beside the concentration and hydrophobicity of the dipeptides, other hydrogel components also influence the foam's stability. Previous studies report that salts have a dramatic effect on the molecular self-assembly of the dipeptides in aqueous media.[22, 24, 32-34] Divalent cations lead to gels with much higher storage moduli *G'* than monovalent cations. In particular, Ca^{2+} leads to a NapFF gel with the highest *G'*, followed by Mg^{2+}, Na^{+} and K^{+}.[24] Since gelation plays an important role in the formation and stability of foams, it is essential to demonstrate how different gels can affect the foam behaviors. To this end, three different salts, $CaCl_2$, $MgSO_4$ and KCl, have been used to induce the gelation. For K^{+}-induced gel, cryo-SEM shows that the fibers in this system are very thin (~10 nm) and do not cross-link with each other to form a network (Figure 2f). Additionally, its *G'* ($<10^2$ Pa, Figure S3b) is smaller than Laplace pressure (~10^3 Pa),[24] which makes bubble coarsening possible. **Figure 6a** shows the foam stabilized by KCl-induced gel. Over a period of one week, the diameters of air bubbles dramatically increased and some of them can even be seen suspended at the bottom of the foam (marked red). The latter supports the idea that a three-dimensional network of dipeptide gel has also been formed even this close to the base of the vial. By recording a 48 hour movie using bright-field microscopy, the change in the diameter of the air bubbles could be observed clearly (Figure 6b and supporting information). No coalescence was observed, demonstrating the important role of the hydrophobic interfacial films around the bubbles. Only large bubbles (diameter >200 μm) expanded. The smaller ones, however, vanished by the end of the movie. This is a coarsening process which involves the transport of gas from the smaller bubbles to the larger bubbles due to the difference in Laplace pressure, and results in an increase in the average bubble diameters with time. **Figure 7** shows the typical coarsening process of foams stabilized by all these three gels. Two average diameters (~100 μm and ~230 μm) have been chosen as

representative small and large bubbles. The foam stabilized by KCl-induced gel exhibits a characteristic coarsening profile, with larger bubbles expanding and smaller ones shrinking; the latter vanish when all of their gas has been transferred to their large neighbors. By contrast, for the foam stabilized by $CaCl_2$-induced gel, no obvious coarsening occurs of either small or large bubbles. In $MgSO_4$-induced system, however, bubbles with both diameters shrank, indicating that *G'* is not sufficiently large to suppress the coarsening for either bubble sizes. The changes in this system are much slower and the bubbles did not vanish quickly; only some very much larger bubbles (diameter >400 μm) slightly increased their sizes. We also prepared foams using $MgCl_2$, see Figure S5; the coarsening behavior was very similar to that for the $MgSO_4$-induced system.

3. Conclusions

We have shown that a bulk NapFF hydrogel, induced by metal cations, can be used to stabilize wet foams for more than two weeks. The foam stability is affected by the concentration of dipeptide and of metal cations. Because of the hydrophobicity of the dipeptides, the fibers, held together by hydrogen bonds, preferentially form interfacial networks. These are involved in stabilizing the air bubbles. Excess molecules self-assemble into a three-dimensional network in the continuous phase, which reduces the amount of drainage and suppresses bubble coarsening. Symbiotically, the presence of the bubbles reduces the amount of phase separation between the hydrogel and the water-rich phase. Three different salts have been used to study the role of metal cations. The foam stabilized by KCl-induced gel shows a typical coarsening process, whereas the bubbles in $CaCl_2$-induced system are very stable. Between these extremes, much slower coarsening has been observed in $MgSO_4$-induced system. These results can be explained by the contribution of the interfacial layers around the bubbles, which suppress the coalescence of touching bubbles, as well as by consideration of the storage modulus of the bulk gel in the

continuous phase. A gel with higher storage modulus can slow down the coarsening and coalescence of the bubbles. This is a simple and scalable method to create a wet foam with long-term stability, which may have potential applications in food, drug delivery and personal care products.

4. Experimental Section

Naphthalene Dipeptide Foaming Solution: At room temperature, NapFF (Figure 1a) was suspended in 2 mL deionized water at concentration of 8 mg/mL. A clear solution can be formed by adding 0.3 mL NaOH (0.1 M aq) upon continuous stirring. This caused a high pH environment for the molecules, and induced aggregation into worm-like micelles in the solution.[30] To study the effect of dipeptide concentration, foaming solutions with 2 mg/mL and 5 mg/mL NapFF molecules were also prepared. Vials with 20 mm diameter and 7.5 cm height are used for all the solutions.

Gelation and Foam Preparation: To form a three-dimensional hydrogel, 0.08 g $CaCl_2 \cdot 2H_2O$ was added into the foaming solution. Gelation has been induced by the Ca^{2+} ions, which lead to the formation of cross-links between different worm-like micelles present in the solution. $CaCl_2 \cdot 2H_2O$ has a powder form; gelation proceeds to completion before the foam preparation. Different amount of $CaCl_2 \cdot 2H_2O$, and another two salts (~0.065 g $MgSO_4$, ~0.08 g KCl) were also used to induce the gelation of the foaming solution.

Foams were prepared by using a Polytron homogenizer (PT-MR 3100) with a 1 cm-diameter head operating at 7000 rpm for one minute. Immediately after preparation, the height of foam is recorded and then measured as a function of time. Before further processing, all samples were stored at room temperature and sealed to prevent liquid evaporation.

Foam Characterization: Confocal microscopy was used to observe the foam samples. A small foam sample was placed on a microscopy slide. The observation was carried out before the sample starts to dry in the air. Thioflavin T (ThT) was used to label self-assembled dipeptide structures. The ThT concentration used was at or below 2 μM to avoid dye self-assembly. Confocal microscopy was performed using a Zeiss Observer.Z1 inverted microscope in conjunction with a Zeiss LSM 700 scanning system 9. A 63× 1.40 NA oil-immersion objective was used to study the fibrous structures in the continuous phase. The ThT fluorescence was excited using the 488 nm line from an Ar-ion laser. A movie of foam stability was taken using an Olympus BX-50 microscope equipped with a QICAM 12-bit Mono Fast 1394 camera (QImaging). Foams were transferred by a pipette and observed inside a sealed observation chamber (4.5mm height).

Naphthalene Fluorescence: The fluorescence spectra from the liquid phase (8 mg/mL NapFF foaming solution with 0.08 g $CaCl_2 \cdot 2H_2O$) were recorded on a Varian Cary Eclipse spectrophotometer. A 3 mL quartz cell with an optical path length of 10 mm was utilized. The solution was excited at 220 nm. The slit width for emission and excitation was 5 nm. The original liquid phase was diluted by deionized water.

Raman measurements: The Raman measurements, in a right angle scattering geometry, were performed using a Coderg T800 triple-grating spectrometer using 514.5 nm excitation (Argon-ion laser). Single spectrum acquisition was between 700 and 2000 cm^{-1} with spectral resolution of 3 cm^{-1} and 1 s integration time. For the measurements, a small amount of foam was deposited on a stainless steel slide and allowed to dry. Prior to beam exposure the sample was cooled to 14°C in a flow of dry nitrogen gas to compensate for laser heating. The laser power was ~150 mW partially focused to ~1 mm diameter. To minimize the interference from the fluorescence

signal, the sample was exposed to the beam for 20 minutes prior to the start of data collection which reduced the fluorescence background to a more steady value. The raw data collected for ten spectra were averaged to obtain the final representation.

Cryo-SEM: Cryogenic scanning electron microscopy (cryo-SEM) was used to visualize the fibrous structures of the self-assembled dipeptides, *i.e.*, the networks around the air bubbles and in the continuous phase. The sample was deposited on a sample holder, frozen in slush nitrogen and transferred to a Gatan Alto 2500 cryostage. Subsequently, the frozen specimen was fractured at −170 ºC, etched for 5 minutes at −90ºC and coated with Au/Pd for 2 minutes. The sample was then transferred to a Hitachi S-4700 scanning electron microscope and was observed using a secondary electrons detector operating at 5.0 kV, at a temperature of −170 ºC.

Rheology. The rheological experiments were performed on a TA Instruments AR 2000 rheometer using a plate-plate geometry (40 mm sand blasted plate, gap 200 µm). Hydrogels and foams of NapFF (8 mg/mL, ~ 4 mL) induced by different salts were prepared and left for 24 hours at room temperature before the measurement. All the samples were carefully scooped onto the rheometer plate. The shear moduli (G' and G'') were measured over a frequency range of 1 -100 rad/s at a strain of 0.5%. All the measurements were carried out at 20 ºC.

Supporting Information

Supporting Information is available from the Wiley Online Library or from the author.

Acknowledgements

We gratefully acknowledge the China Scholarships Council/ University of Edinburgh Scholarship for Tao Li and the EPSRC for support via grant EP/J007404/1.

Received: ((will be filled in by the editorial staff))
Revised: ((will be filled in by the editorial staff))
Published online: ((will be filled in by the editorial staff))

[1] F. Carn, A. Colin, M.-F. Achard, H. Deleuze, C. Sanchez, R. Backov, *Adv. Mater.* **2005**, *17*, 62.

[2] A. L. Campbell, S. D. Stoyanov, V. N. Paunov, *Soft Matter* **2009**, *5*, 1019.

[3] F. Carn,; H. Saadaoui, P. Masse, S. Ravaine, B. Julian-Lopez, C. Sanchez, H. Deleuze, D. R. Talham, R. Backov, *Langmuir* **2006**, *22*, 5469.

[4] U. T. Gonzenbach, A. R. Studart, E. Tervoort, L. J. Gauckler, *Angew. Chem., Int. Ed*. **2006**, *45*, 3526.

[5] E. Rio, W. Drenckhan, A. Salonen and D. Langevin, *Adv. Colloid Interface Sci.*, **2014**, *205*, 74.

[6] I. D. Morrison, S. Ross, *Colloidal Dispersions: Suspensions, Emulsions, and Foams*; Wiley-Interscience: New York, **2002**.

[7] A. B. Subramaniam, C. Mejean, M. Abkarian, H. A. Stone, *Langmuir* **2006**, *22*, 5986.

[8] H. A. Wege, S. Kim, V. N. Paunov, Q. Zhong, O. D. Velev, *Langmuir* **2008**, *24*, 9245.

[9] B. P. Binks, R. Murakami, *Nat. Mater.* **2006**, *5*, 865.

[10] A. F. Dexter, A. S. Malcolm, A. P. J. Middelberg, *Nat. Mater.* **2006**, *5*, 502.

[11] P. Ptaszek, *Food Res. Int.* **2013**, *54*, 478.

[12] J. C. Banach, Z. Lin, B. P. Lamsal, *LWT−Food Sci. Technol.* **2013**, *54*, 397.

[13] C. van der Ven, H. Gruppen, D. B. A. de Bont, A. G. J. Voragen, *Journal of Agricultural and Food Chemistry*, **2002**, *50*, 2938.

[14] J. P. Davis, D. Doucet, E. A. Foegeding, *J. Colloid Interface Sci.* **2005**, *288*, 412.

[15] A. F. Dexter, A. P. J. Middelberg, *J. Phys. Chem. C* **2007**, *111*, 10484.

[16] P. W. J. R. Caessens, H. Gruppen, S. Visser, G. A. van Aken, A. G. J. Voragen, *J. Agric. Food Chem.***1997**, *45*, 2935.

[17] K. K. Agyare, K. Addo, Y. L. Xiong, *Food Hydrocolloids* **2009**, *23*, 72.

[18] A. S. Malcolm, A. F. Dexter, A. P. J. Middelberg, *Soft Matter* **2006**, *2*, 1057.

[19] A.P.J. Middelberg, M. Dimitrijev-Dwyer, *Chem Phys Chem* **2011**, *12*, 1426.

[20] T. Li, M. Kalloudis, A. Z. Cardoso, D. J. Adams, P. S. Clegg, *Langmuir* **2014**, *30*, 13854.

[21] S. Bai, C. Pappas, S. Debnath, P.W.J.M. Frederix, J. Leckie, S. Fleming, R.V. Ulijn, *ACS Nano*, **2014**, *8*, 7005.

[22] J. F. Shi, Y. Gao, Y. Zhang, Y. Pan, B. Xu, *Langmuir* **2011**, *27*, 14425.

[23] Z. Yang, G. Liang, M. Ma, Y. Gao, Y., B. Xu, *J. Mater. Chem.*, **2007**, *17*, 850.

[24] L. Chen, G. Pont, K. Morris, G. Lotze, A. Squires, L. C. Serpell, D. J. Adams, *Chem. Commun.* **2011**, *47*, 12071.

[25] Y. Zhang, Y. Kuang, Y. Gao, B. Xu, *Langmuir*, **2011**, *27*, 529.

[26] J. M. Jung, D. Z. Gunes, R. Mezzenga, *Langmuir* **2010**, *26*, 15366.

[27] L. G. Tensmeyer, E. W. Kauffman in *Spectroscopic Methods for Determining Protein Structure in Solution*, Ed. H. A. Havel, VCH, New York, **1996**, Ch. 5.

[28] H. Shinohara, Y. Yamakita, K. Ohno, *J. Mol. Struct.* **1998**, *442*, 221.

[29] C. Xie, Y.-q. Li, W. Tang, R.J. Newton, *J. Appl. Phys*. **2003**, *94*, 6138.

[30] L. Chen, T. O. McDonald, D. J. Adams, *RSC Adv.* **2013**, *3*, 8714.

[31] D. J. Durian, D. A. Weitz, D. J. Pine, *Science,* **1991**, *252*, 686.

[32] J. J. Panda, A. Mishra, A. Basu, V. S. Chauhan, *Biomacromolecules* **2008**, *9*, 2244.

[33] S. Roy, N. Javid, P. Frederix, D. A. Lamprou, A. J. Urquhart, N. T. Hunt, P. J. Halling, R. V. Ulijn, *Chem.–Eur. J.*, **2012**, *18*, 11723.

[34] S. Fleming, R.V. Ulijn, *Chem. Soc. Rev.* **2014**, *43*, 8150.

Figure 1. A wet foam stabilized by NapFF hydrogel. (a) NapFF molecule used in this study. (b) NapFF solution (8 mg/mL); (c) NapFF hydrogel induced by $CaCl_2 \cdot 2H_2O$ (35 mg/mL); (d) a freshly prepared foam; (e) the foam one week after preparation; (f) the foam two weeks after preparation. (g) Foam extruded with a pipette. (h) Response of the foam to oscillating shear plotted in the form of storage and loss moduli as a function of oscillation frequency. A foam of NapFF (8 mg/mL, 2 mL) induced by $CaCl_2 \cdot 2H_2O$ (35 mg/mL) was prepared and left for 24 hours at room temperature before the measurement.

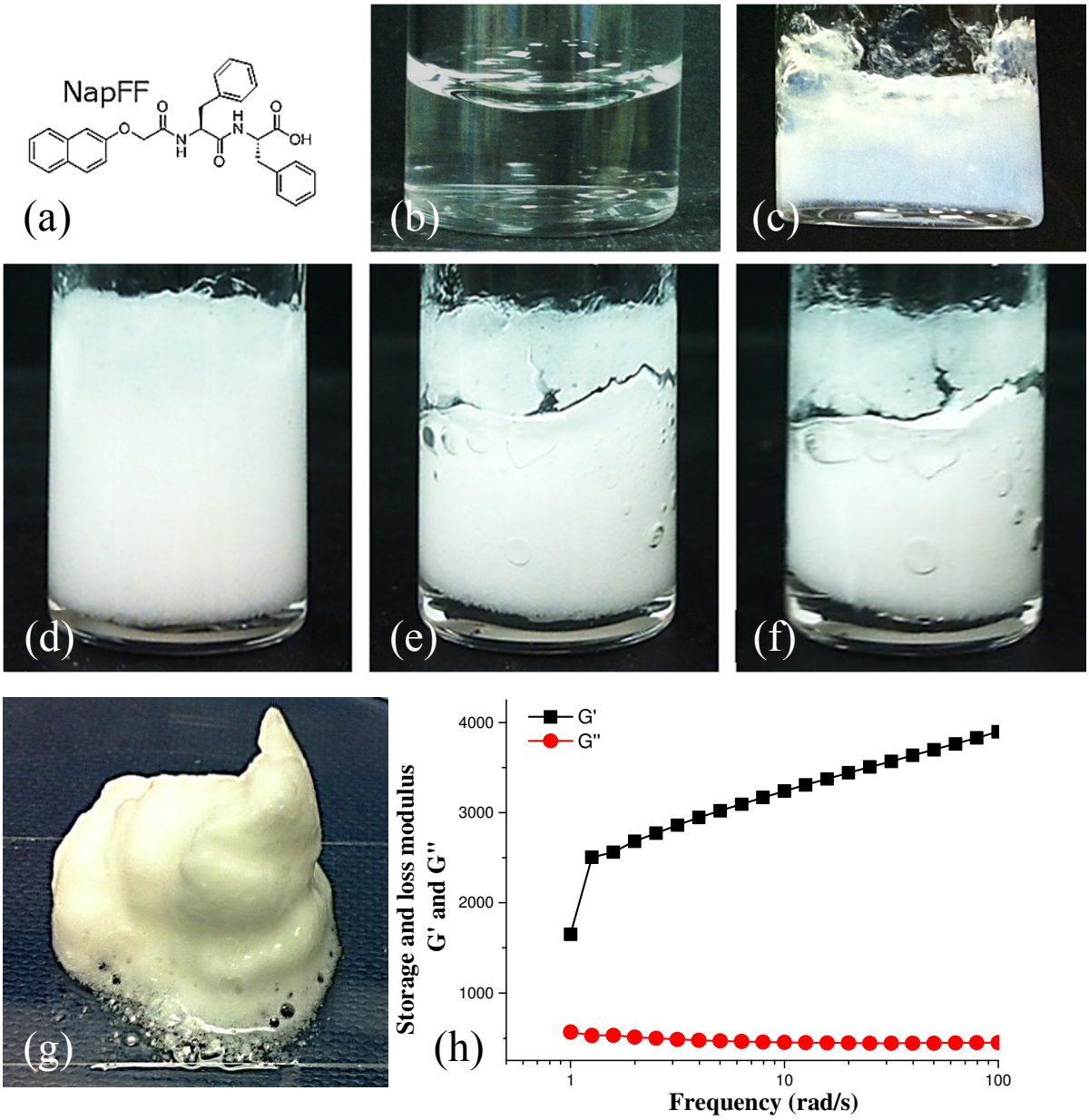

Figure 2. (a) Cryo-SEM image of the hydrogel networks stabilizing the foam shown in Figure 1b. (b) Interfacial networks around the air bubbles (marked red in (a)) showing the organization of the strands with great clarity. Scale bar is 5 µm. (c) The fibrous structures of the dipeptide aggregations in the continuous phase (marked blue in (a)). The scale bar is 10 µm. (d-f) Cryo-SEM images of different foam systems. The scale bars are 1 µm. (d) 8 mg/mL NapFF with 35 mg/mL $CaCl_2 \cdot 2H_2O$; (e) 2 mg/mL NapFF with 35 mg/mL $CaCl_2 \cdot 2H_2O$; (f) 8 mg/mL NapFF with 35 mg/mL KCl. (g) Confocal image of the air bubbles in the wet foam. The dipeptide is dyed using ThT. (h) Raman spectrum of the self-assembled dipeptide molecules in the foam following drying on a metal substrate.

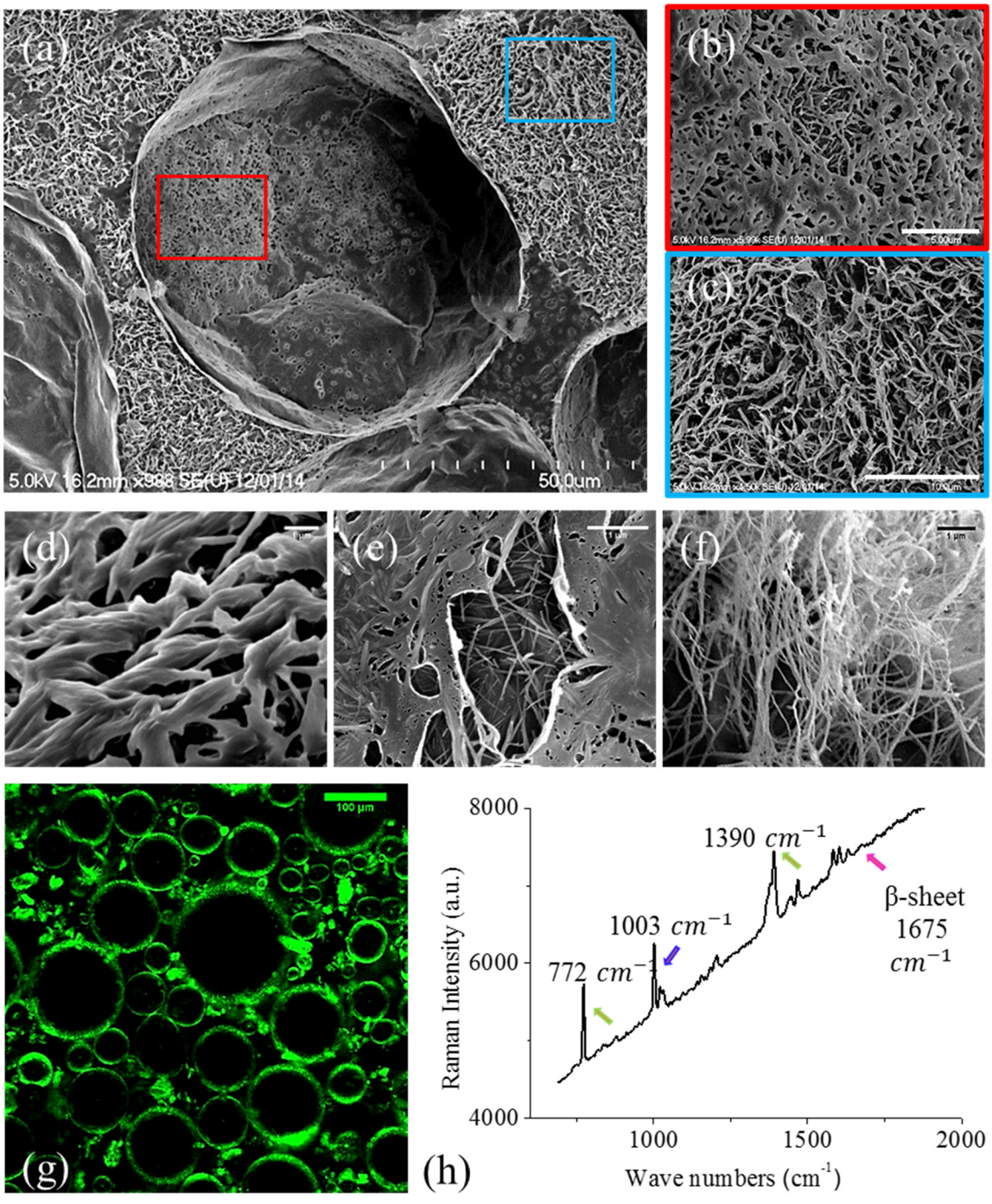

Figure 3. The effect of dipeptide concentration on the foam stability. Foams are stabilized by NapFF gel with 5 mg/mL (a) and 2 mg/mL (b) dipeptide, respectively. Both samples have the same amount (35mg/mL) of $CaCl_2 \cdot 2H_2O$. Drainage can be observed after one week of foam formation. From left to right: freshly prepared foam; one week after preparation; two weeks after preparation. (c) Confocal images of the air bubbles in foam (a). During the drainage process, the bubbles distort and adopt non-spherical shapes, and the hydrogel in the continuous phase becomes more visible. From left to right: freshly prepared foam; two weeks after preparation; 50 days after preparation.

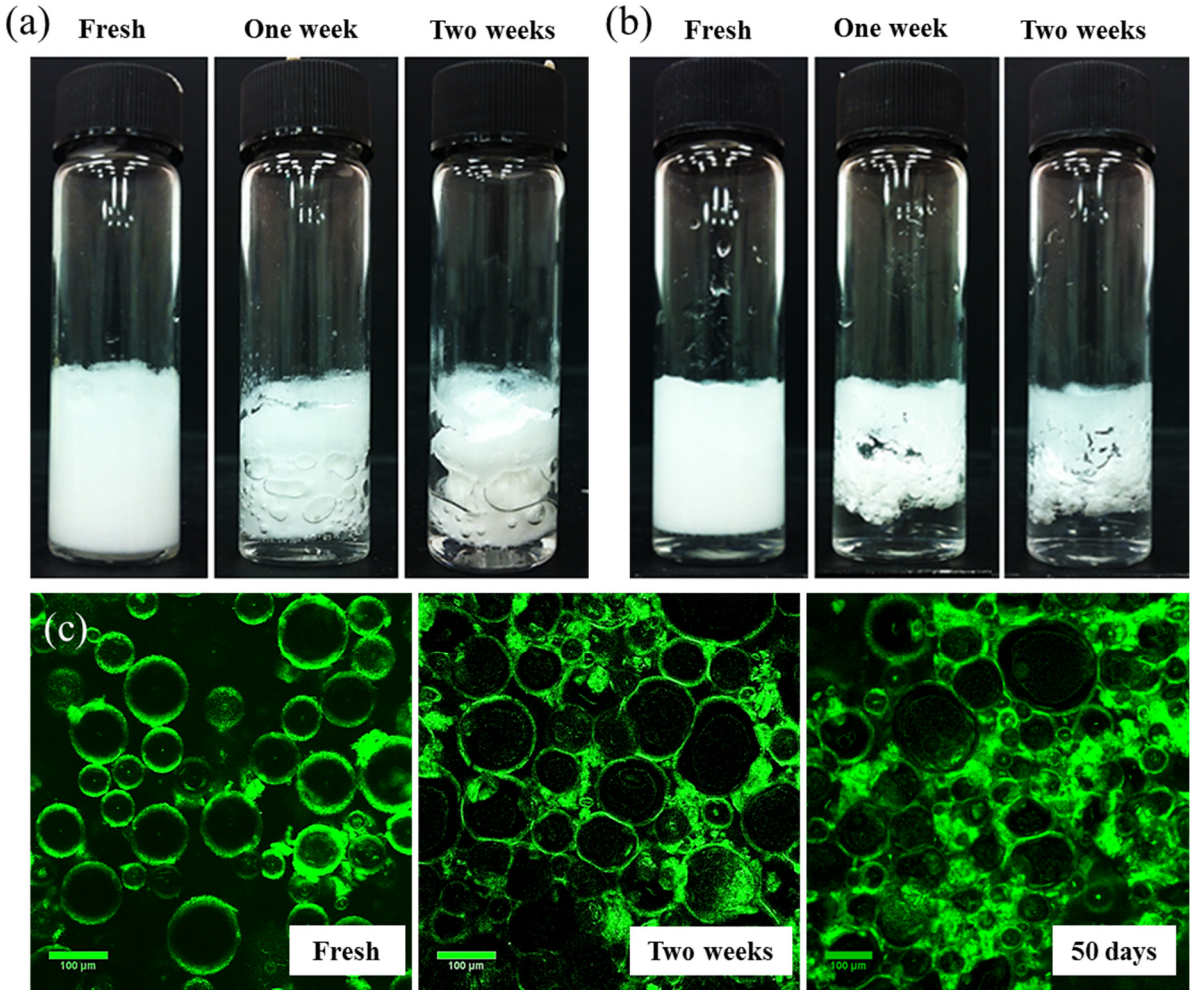

Figure 4. The effect of metal ion concentration on the foam stability. (a) Time dependence of the height of foams with different amount of $CaCl_2 \cdot 2H_2O$; as concentrations these are 35 mg/mL, 17 mg/mL and 4.4 mg/mL, respectively. (b, c) Foam stabilized by 8 mg/mL NapFF with 0.04 g and 0.01 g $CaCl_2 \cdot 2H_2O$, respectively. Both photographs were taken one week after the formation of the foam.

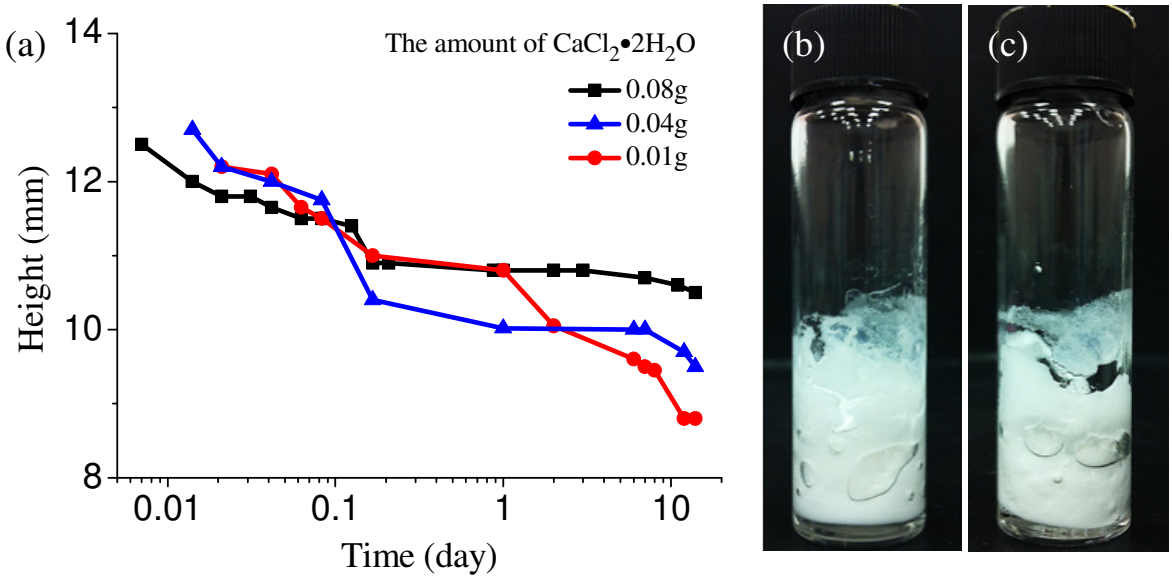

Figure 5. Hydrogel (no bubbles) with (a-c) different concentrations of NapFF and $CaCl_2 \cdot 2H_2O$ (d, e) using $MgSO_4$. 2 mL NapFF solution were used for all the samples. (a-c) The red dashed line indicates the total sample volume prior to inversion; the remainder of the sample volume is liquid and has descended out of the images. There is an obvious decrease in hydrogel volume with decreasing the concentration of NapFF or Ca^{2+}. (a) 8 mg/mL NapFF with 35 mg/mL $CaCl_2 \cdot 2H_2O$, the gel height is 9.1 mm. (b) 8 mg/mL NapFF with 4.4 mg/mL $CaCl_2 \cdot 2H_2O$, the gel height is 7.5 mm. (c) 2 mg/mL NapFF with 35 mg/mL $CaCl_2 \cdot 2H_2O$, the gel height is 3 mm. All the samples are two weeks after preparation. Some further shrinkage is observed over a timescale of months. (d) NapFF (8 mg/ml) gelation induced by 28 mg/mL $MgSO_4$ two weeks after preparation; (e) six months after preparation; inset showing the extent of shrinkage.

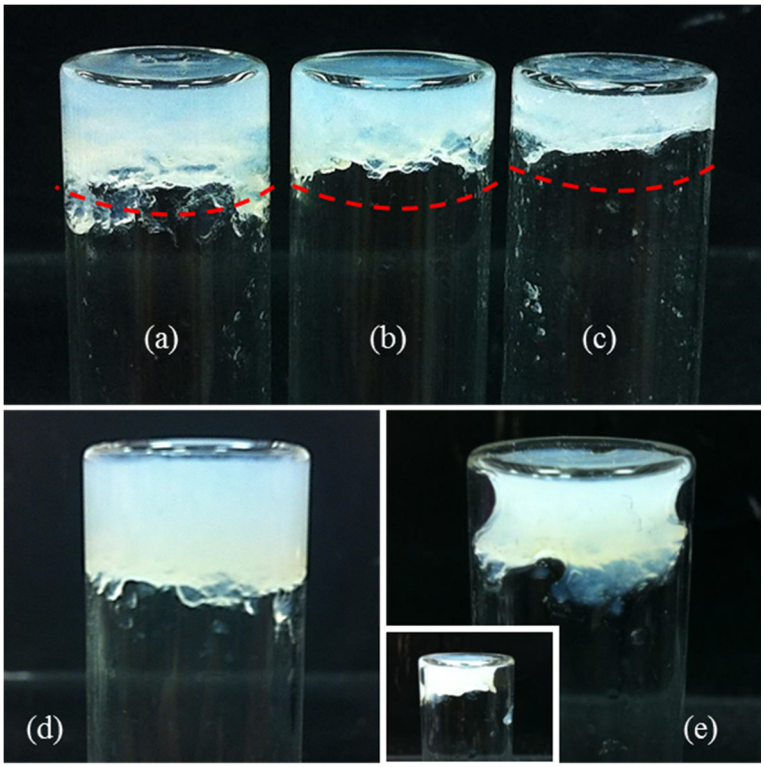

Figure 6. (a) Short-lived foam stabilized by KCl-induced gel. From left to right: freshly prepared foam; two days after preparation; one week after preparation. Bubbles suspended at the bottom of the foam are marked by the red ellipse. (b) Bright-field images of the air bubbles in foam (a) for 48 hours. Larger bubbles expand (marked red) whereas smaller ones shrink to vanish (marked yellow). The scale bar is 200 μm.

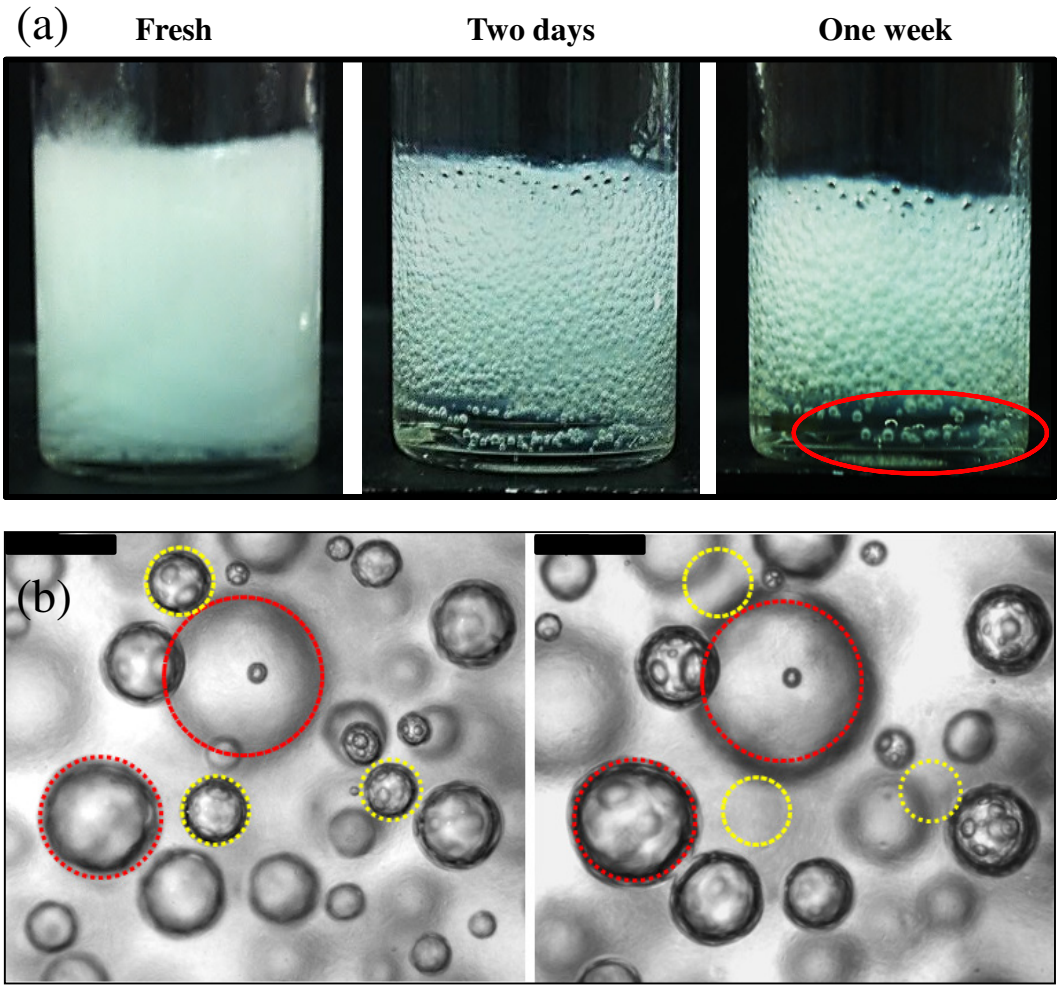

Figure 7. Time dependence of the diameter of typical bubbles stabilized by different gels. (a) Bubbles with large diameter (~230 µm). (b) Bubbles with smaller diameter (~100 µm).

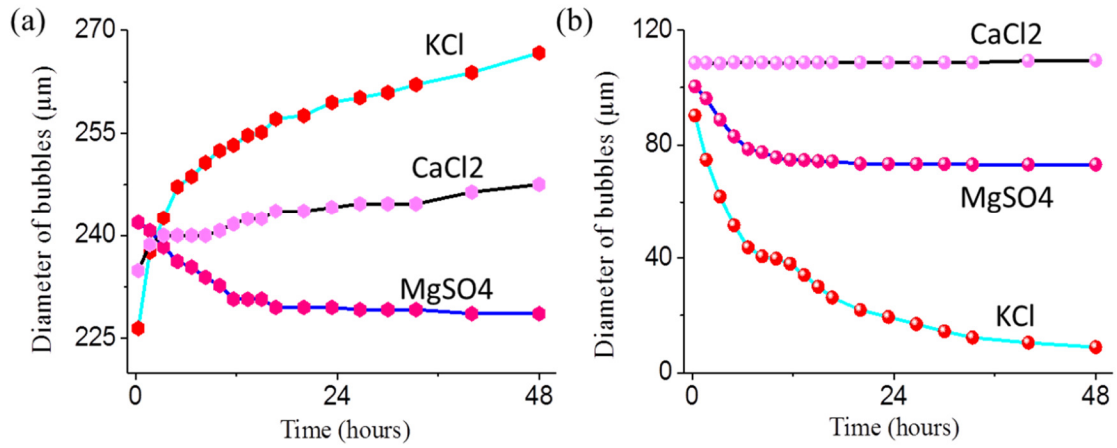

Author Photograph(s) ((40 mm broad, 50 mm high, gray scale))

A wet foam system with long-term stability can be stabilized by a hydrophobic dipeptide hydrogel. The dipeptide molecules preferentially self-assemble into interfacial films to protect the air bubbles. Excess molecules form a three-dimensional network in the continuous phase, which reduces drainage and suppresses bubble coarsening. The concentration and storage modulus of the hydrogel can affect the foam stability.

Keyword: supramolecular materials, dipeptide fibers, hydrogel, self-assembly

T. Li, F. Nudelman, J. W. Tavacoli, H. Vass, D. J. Adams, A. Lips and P. S. Clegg*

Long-Lived Foams Stabilized by a Hydrophobic Dipeptide Hydrogel

ToC figure ((Please choose one size: 55 mm broad × 50 mm high **or** 110 mm broad × 20 mm high. Please do not use any other dimensions))

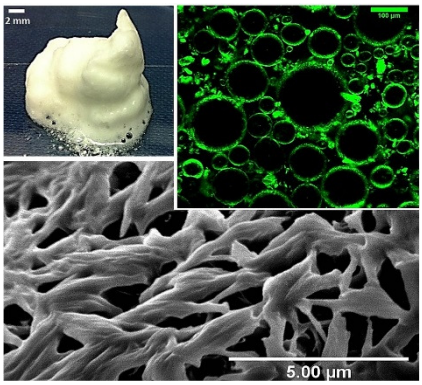

Supporting Information

Long-Lived Foams Stabilized by a Hydrophobic Dipeptide Hydrogel

Tao Li, Fabio Nudelman, Joe W. Tavacoli, Hugh Vass, Dave J.Adams, Alex Lips and Paul S. Clegg*

T. Li, Dr J.W. Tavacoli, H. Vass, Prof. A. Lips, Dr. P.S. Clegg
School of Physics and Astronomy, University of Edinburgh, Peter Guthrie Tait Road, Edinburgh EH9 3FD, UK
E-mail: paul.clegg@ed.ac.uk
Dr. F. Nudelman,
School of Chemistry, University of Edinburgh, Joseph Black Building, David Brewster Road, Edinburgh EH9 3FJ, UK.
Prof. D. J. Adams,
Department of Chemistry, University of Liverpool, Crown Street, Liverpool, L69 7ZD, UK

The Foam-Ability of NapFF Solution

NapFF solution (pH ≈ 10.0) was used as a foam stabilizer at a high concentration. A foam can be created by aerating the solution with a Polytron homogenizer (Figure S1b). However, this foam is not stable and vanishes within two hours (Figure S1g).

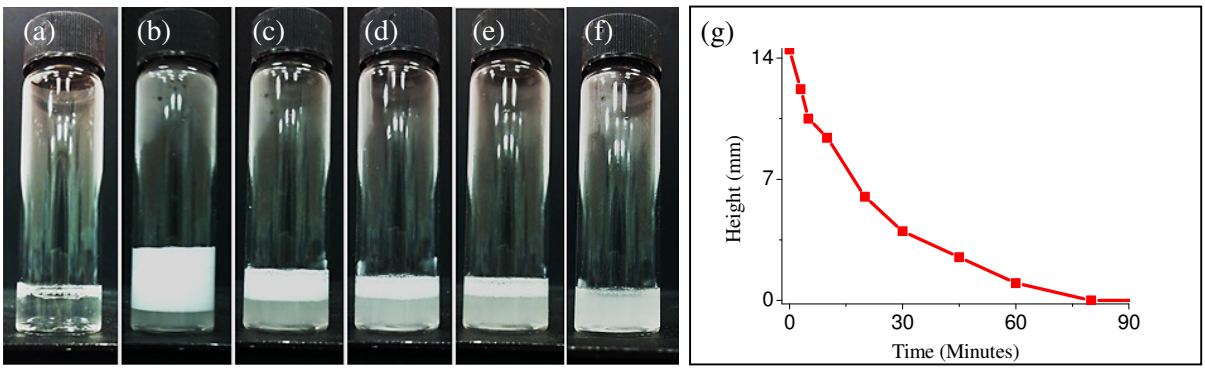

Figure S1. The foamability of NapFF solution (8 mg/mL) without gelation. (a) New solution before aerating; (b) 3 minutes (c) 20 minutes (d) 30 minutes (e) 45 minutes and (f) 90 minutes after aerating. (g) Time dependence of the height of foam.

Naphthalene Fluorescence

Figure S2 shows the naphthalene fluorescence from the liquid phase at the bottom of the foam (8 mg/mL NapFF foaming solution with 0.08 g $CaCl_2 \cdot 2H_2O$). The fluorescence signal is very strong even after diluting 100 times, which means there are some excess NapFF molecules in the liquid phase.

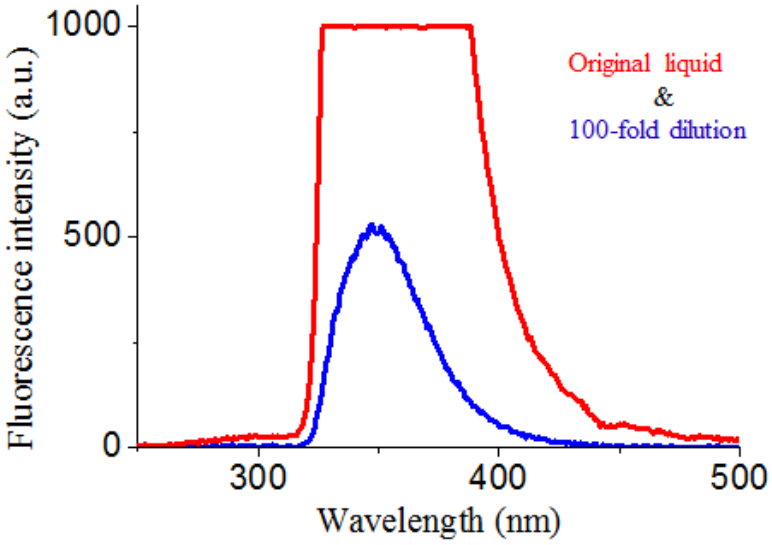

Figure S2. The Naphthalene fluorescence signal measured from the drained liquid phase. The red curve is from the original liquid, and the blue curve is from a 100-fold dilution.

The Rheological Properties of the Gel

Gelled dipeptide exists in the continuous phase between bubbles. A comparison of the rheological properties of the gel, Figure S3, with the Laplace pressure of the bubbles (see main text) gives an indication of the role of the gel in stabilizing the bubbles. The results indicate the very large difference between hydrogels induced using divalent and monovalent ions. This difference is reflected in the stability of the resulting foams.

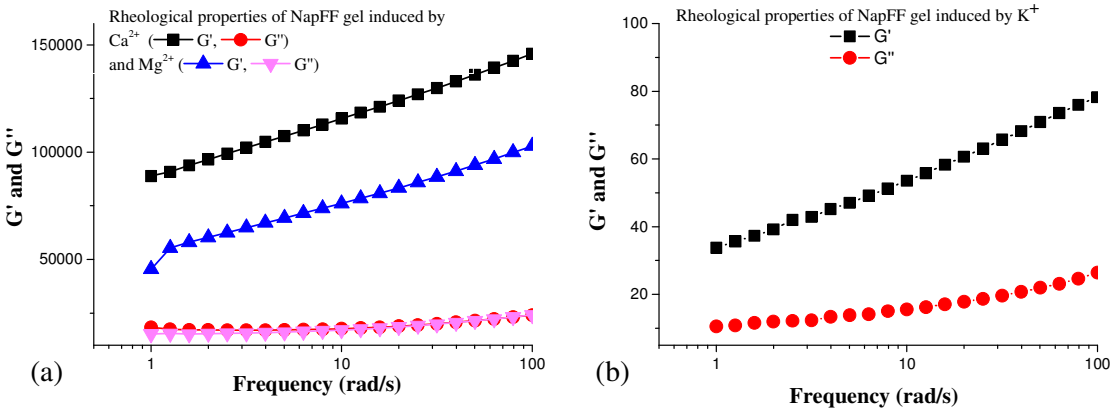

Figure S3. Showing the response of the gel (without bubbles) to oscillating shear. Here the oscillation amplitude is 0.5% strain and the frequency is varied from 1-100 rad/s. Hydrogels of NapFF (8 mg/mL, 4 mL) induced by different salts were prepared and left 24 hours at room temperature before the measurement. (a) Storage, G', and loss, G", moduli for gels induced using Ca^{2+} and Mg^{2+} ions (b) Storage and loss module for gels induced using K^{+} ions.

The Foam-Ability of BrNapAV Dipeptides

Previous studies show that BrNapAV can form spherical aggregates in solution at high pH, which cannot self-assemble into a fiber-like network.[1] Similar spherical aggregates (~20 µm) have also been observed in the foam experiments (Figure S4). This can be caused by the hydrophobicity of BrNapAV, which is quite hydrophilic and their aggregates cannot stay at the air-water interface.

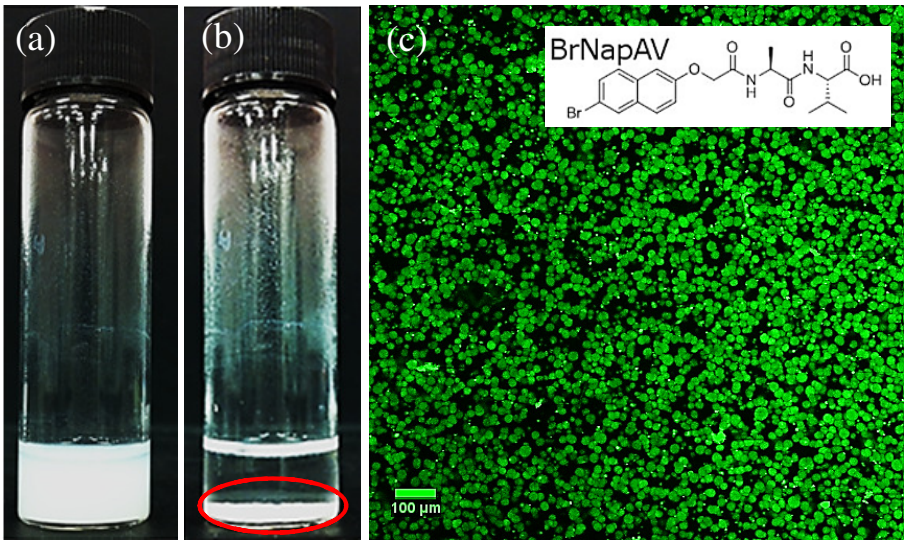

Figure S4. (a, b) BrNapAV dipeptides cannot stabilize a wet foam. (c) Fluorescence confocal microscopy of the sediments with ThT in (b). These particles might involve the salt at high concentration. The inset shows the BrNapAV molecule used in this study.

The influence of the counter ions

Figure S5 shows a foam stabilized using a dipeptide hydrogel which was induced using $MgCl_2$. The hydrogel was prepared using 2ml of 8mg/ml NapFF together with 0.52g $MgCl_2$. The foam characteristics are very similar to the $MgSO_4$-induced system discussed in the main text.

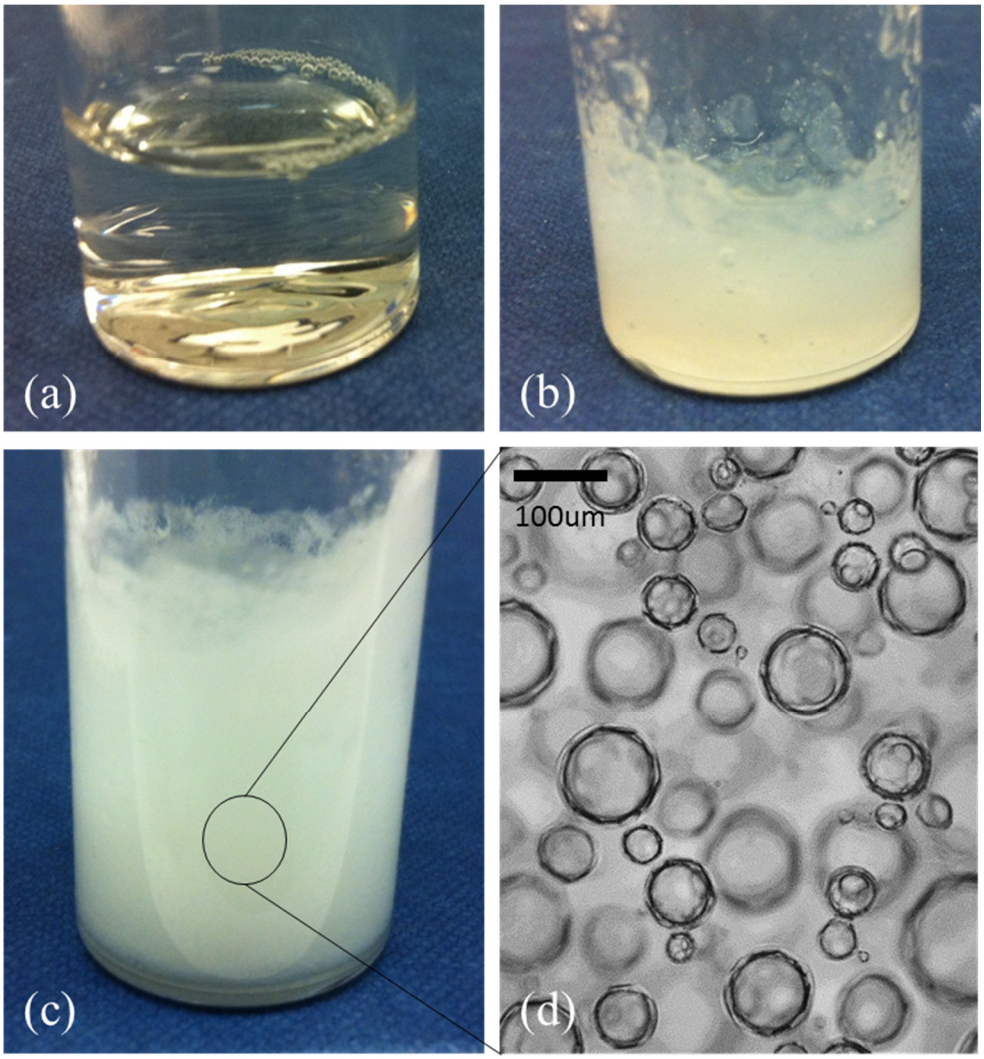

Figure S5. (a) The dispersion of NapFF prior to the addition of salt. (b) The hydrogel formed due to the addition of $MgCl_2$. (c) A macroscopic image of the resulting foam. (d) A bright field image of the bubbles in the foam. They exhibit a slight reduction in size with time in a similar way to the $MgSO_4$-induced system.

A film of the coarsening process of the foam stabilized by KCl-induced gel is also available in supporting information.

[1] L. Chen, G. Pont, K. Morris, G. Lotze, A. Squires, L. C. Serpell, D. J. Adams, *Chem. Commun.* **2011**, *47*, 12071.